

Local entropy and structure in a two-dimensional frustrated system

Matthew D. Robinson,^{1,2,a)} David P. Feldman,^{3,4,b)} and Susan R. McKay^{2,c)}

¹Red Shift Company LLC, 1017 E. South Boulder Road, Suite F, Louisville, Colorado 80027, USA

²Department of Physics and Astronomy, University of Maine, Orono, Maine 04469, USA

³College of the Atlantic, Bar Harbor, Maine 04609, USA

⁴Santa Fe Institute, 1399 Hyde Park Road, Santa Fe, New Mexico 87501, USA

(Received 13 October 2010; accepted 17 May 2011; published online 30 September 2011)

We calculate the local contributions to the Shannon entropy and excess entropy and use these information theoretic measures as quantitative probes of the order arising from quenched disorder in the diluted Ising antiferromagnet on a triangular lattice. When one sublattice is sufficiently diluted, the system undergoes a temperature-driven phase transition, with the other two sublattices developing magnetizations of equal magnitude and opposite sign as the system is cooled.¹ The diluted sublattice has no net magnetization but exhibits spin glass ordering. The distribution of local entropies shows a dramatic broadening at low temperatures; this indicates that the system's total entropy is not shared equally across the lattice. The entropy contributions from some regions exhibit local reentrance, although the entropy of the system decreases monotonically as expected. The average excess entropy shows a sharp peak at the critical temperature, showing that the excess entropy is sensitive to the structural changes that occur as a result of the spin glass ordering. © 2011 American Institute of Physics. [doi:10.1063/1.3608120]

How do physical and natural systems store, transmit, and manipulate information across space and time to produce patterns? How is information processing embedded in spatially extended dynamical systems? These matters are of interest to those wishing to design novel computational devices. After all, all practical computation must be physically embodied. Moreover, analyzing a system in terms of its information processing capabilities is a way to discover organization and regularity—one of the central goals of science. We show how well understood measures of information and memory can be adapted and applied to a heterogeneous two-dimensional system. In particular, we analyze a model in which variables interact on a regular triangular lattice. The interactions are such that it is energetically favorable for variables to take on opposite values, but the geometry of the lattice does not allow this to occur. Such systems are said to be *frustrated*. We study a model in which sites are deleted, which has the effect of partially relieving frustration. The result is a transition to an ordered state as the temperature is lowered. The nature of this ordering is probed by means of the local measures of information and memory. Our results show that entropy and memory may be viewed as local quantities that are unevenly shared across the lattice. We argue that these local quantities are a powerful and broadly applicable tool for understanding information processing in heterogeneous systems.

I. INTRODUCTION

The question of how physical objects compute has gained considerable attention over the years. That is, how does a system store, transform, and manipulate information? And how can these properties be inferred from observations? Since the 1980's, there has been considerable work aiming to develop ways of answering these questions. The result of this work is a well understood set of quantities that measure computation, memory, information, and unpredictability, for one-dimensional (1D) systems. For reviews, see Refs. 2–7. The situation in two dimensions is not as settled. Many of the measures of computation and information introduced for 1D systems do not generalize in a unique way to two-dimensional (2D) systems. And the combinatorial explosion associated with two-dimensional patterns poses a challenge for numerical estimation of information processing measures. Nevertheless, there is a growing body of work that aims to develop approaches to information and computation in two dimensions. See Ref. 8 and references therein; for more recent work see Refs. 9–14.

In this work, we apply information theoretic measures to a disordered lattice model which shows spin-glass ordering at low temperatures. Spin glass models were originally devised to describe disordered magnetic materials, but subsequently have been used to model a wide range of phenomena in which entities interact through random interactions and/or exhibit frustration. Researchers have also made connections between spin glasses and a number of information processing phenomena, including neural networks, associative memory, and error correcting codes.¹⁵

Fully characterizing, the nature of the ordering that occurs in models of disordered magnetic systems has been a long-standing challenge in statistical physics. In particular,

^{a)}Electronic address: matthewd@mailaps.org.

^{b)}Electronic address: dpf@santafe.edu.

^{c)}Electronic address: susan.mckay@umit.maine.edu.

understanding the low-temperature behavior of two-dimensional spin glasses has been a topic of considerable interest in the last decade.^{16–20} In general, the onset of spin-glass ordering is usually associated with broken ergodicity, where the phase space of the system is divided into several (or perhaps many) distinct regions with boundaries across which the system cannot pass with finite probability in the thermodynamic limit. Unlike non-glassy transitions, it is generally believed that these regions of phase space are not related by any simple symmetry operation, such as a global spin flip or a global spin rotation.

One manifestation of this loss of ergodicity is that the system loses spatial translation symmetry. For example, in many glassy systems below the transition point, the local magnetization no longer equals the global magnetization. Typically, the global magnetization remains zero, while individual spins acquire a non-zero expectation value. The magnetization is no longer the same on all the sites. The extent by which the magnetization differs from site to site can be measured by the Edward-Anderson order parameter, as discussed more fully below.

In this work, we show that a similar scenario holds for the entropy. To do so, we make use of an information-theoretic method for calculating the entropy. This approach, whose accuracy is well established for pure systems,^{21–29} allows one to express the entropy of the lattice as a function of the frequencies of occurrence of configurations in a small neighborhood of spins. These frequencies can be directly measured in a Monte Carlo simulation, avoiding the necessity of thermodynamic integration to calculate the entropy.

This information theoretic method allows one to define and measure local entropies—the ensemble average of the spatial entropy at a particular site. Thus, we can decompose the entropy into its local contributions, just as we can decompose the global magnetization into local contributions. This gives us a direct view of the extent to which the disorder in the system leads to spatial fluctuations in entropy. In so doing, we obtain a novel way to characterize the changes in spatial structure that occur in a glassy system. We also calculate a local form of the two-dimensional excess entropy, a measure of the spatial structure or memory of a system. We present the results of applying our method to a two-dimensional lattice model recently introduced by Kaya and Berker¹ and discussed below.

Our results add to a growing body of recent work^{10–12,14,30} on local information measures—i.e., measures that are applied to a spatially extended system but which measure some aspect of the information processing that is occurring at a particular lattice site. In the extant work on local information measures, information is localized as a result of random initial conditions. The rules governing the system are homogeneous, but localized structures form as a result of the random initial configuration used to seed the process. In contrast, in the system we study here the localization of information processes arises as a result of spatial heterogeneities in the dynamics of the lattice variables which, in turn, is a result of the random site dilution in the model.

Our paper is organized as follows. We begin in Sec. II by reviewing the Kaya-Berker model. In Sec. III, we discuss

our methods in considerable detail. We then present our results in Sec. IV and conclude in Sec. V by highlighting several key points and suggesting several areas for future work.

II. THE KAYA-BERKER MODEL

The model we will work with is a variant of the two-dimensional anti-ferromagnetic Ising model on a triangular lattice. The Hamiltonian (or energy function) for the model is given by

$$\mathcal{H} = -J \sum_{\langle ij \rangle} S_i S_j, \quad (1)$$

where the sum is understood to be only over sites that are nearest neighbors. Since the model is on a triangular lattice, each site has six nearest neighbors. Each spin S_i is a binary variable: $S_i \in \{-1, +1\}$.

In the following, we will fix the coupling constant J at -1 . Hence, it is energetically favorable for neighboring spins to anti-align. However, the geometry of the system does not allow for all spins to anti-align with their neighbors. This phenomenon, wherein all energetic constraints cannot be simultaneously satisfied, is known as frustration. In fact, this system is maximally frustrated. On every triangle of adjoining spins, it is impossible to have all spins anti-aligned with their neighbors. As a result of this geometric frustration, the system does not order at finite temperature.³¹

Grest and Gabl³² studied a variant of this model in which sites are randomly deleted. They obtained Monte Carlo results suggesting that the antiferromagnet will exhibit long-range, spin-glass ordering in the presence of quenched random dilution. Specifically, Grest and Gabl report that a non-vanishing quenched dilution gives rise to a second order phase transition. This phenomenon is discussed in general terms in Ref. 33. For follow-up work on Grest and Gabl's model, see Refs. 34–37.

A triangular lattice decomposes naturally into three sublattices such that sites in a given sublattice are neighbored only by sites in the other two sublattices, as illustrated in Fig. 1. Kaya and Berker¹ analyzed a model in which sites are randomly diluted only on one sublattice. We shall refer to

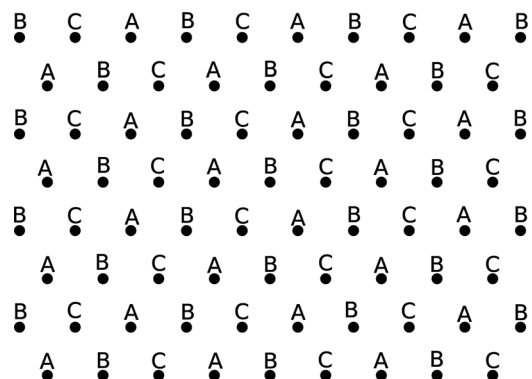


FIG. 1. The triangular lattice decomposed into three sublattices, denoted A, B, and C. Each site, indicated with the solid dot, has six nearest neighbors. Note that each site is not neighbors with any other sites on the same sublattice. For example, all sites on sublattice A have neighbors from sublattices B and C only, and not A.

the lattice on which dilution occurs as sublattice A; the other two sublattices are B and C. We measure dilution strength as the percent of the sites diluted on sublattice A. Thus, a dilution of 100% corresponds to a lattice in which sublattice A is deleted entirely, resulting in a honeycomb lattice.

Kaya and Berker,¹ using a combination of hard-spin mean field theory^{38,39} and Monte Carlo simulations, analyzed this model. They found that the model orders at finite temperature at a dilution strength at or above approximately 9.75%. The nature of this order is as follows: sublattices B and C spontaneously magnetize with opposite signs and equal magnitudes, and there is spin-glass ordering on sublattice A as indicated by a non-zero value of the Edwards-Anderson (EA) order parameter, to be defined below. Physically, the addition of vacancies to the two-dimensional case relieves frustration and leads to this ordered phase.¹ Thus, this model system provides an example of order arising from disorder and offers a generic system to explore the interplay between geometric frustration and randomness. This system exhibits spin-glass and magnetic ordering on separate sublattices, so its phase diagram possesses an unusual richness for a two-dimensional, short-range model. We shall refer to this model below as the Kaya-Berker model.

III. METHODS AND BACKGROUND

The central quantity in our study, the entropy, has a dual existence. In thermodynamics, it is a macroscopic state variable that measures the extent to which a system's internal energy cannot be used to perform work. Entropy may also be viewed from the point of view of information theory or statistical mechanics. In this view, the entropy is a measure of the disorder of the microstate. The entropy tells us the amount of memory needed, on average, to store successive measurements of the system's configuration. We will make use of both views of entropy below.

A. Thermodynamic entropy and other thermodynamic quantities

The entropy is a thermodynamic state variable and can be calculated by integrating $ds = (c/T)dT$, where s is the entropy density, c the specific heat per occupied site, and T the temperature. (Here and throughout, we take Boltzmann's constant equal to one.) In practice, to estimate the entropy density s in a Monte Carlo simulation, one usually integrates ds from a temperature at which the entropy is known exactly. Often, this is the infinite temperature limit, where s is $\ln 2$, since all configurations are equally likely as $T \rightarrow \infty$. In this case, we have the following expression for the entropy density s as a function of the temperature T :

$$s(T) = \ln 2 - \int_{\infty}^T \frac{c(T')}{T'} dT'. \quad (2)$$

We shall refer to this quantity as the *thermodynamic entropy* since this form of $s(T)$ is obtained by the thermodynamic relationship $du = Tds$, where u is the internal energy density.

The specific heat c relates changes in an object's temperature T to changes in its internal energy density u :

$du = cdT$. It can also be related to the fluctuations in the internal energy

$$c = \beta^2 \langle (u - \langle u \rangle)^2 \rangle, \quad (3)$$

where the angular brackets indicate a thermal expectation value,

$$\langle \cdot \rangle \equiv \sum_i \cdot e^{-\beta E_i}, \quad (4)$$

and β is the inverse temperature.

The magnetization m is defined as the expectation value of the spin variables

$$m \equiv \langle \sum_i S_i \rangle. \quad (5)$$

One can also define a local magnetization, which is simply the expectation value of a spin at a particular site i

$$m_i = \langle S_i \rangle. \quad (6)$$

One type of ordering displayed by models of magnetic materials occurs when the system undergoes a transition from zero to non-zero magnetization. Such a transition does not occur in the frustrated model studied here, however, since the competing interactions do not allow for a net magnetization. However, for some frustrated systems, as the temperature is lowered the spins "freeze in" locally, and the local magnetizations are non-zero. This sort of state is known as a spin glass. Spin glass ordering is often measured via the EA order parameter q

$$q \equiv \frac{1}{N} \sum_i m_i^2. \quad (7)$$

That is, the EA order parameter q is the average of the square of all of the local magnetizations in the system. The EA order parameter is non-zero when the glass state is entered and spins locally freeze into a fixed value.

B. Information-theoretic entropy

The entropy may also be expressed via the Gibbs formula or, equivalently, by using the *Shannon entropy* $H[X]$ of a random variable X . Specifically, let X be a random variable that assumes the values $x \in \mathcal{X}$, where \mathcal{X} is a finite set. We denote the probability that X assumes the particular value x by $\text{Pr}(x)$. The *Shannon entropy* of the random variable X is defined by

$$H[X] \equiv - \sum_{x \in \mathcal{X}} \text{Pr}(x) \log_2 \text{Pr}(x). \quad (8)$$

The entropy $H[X]$ measures the average uncertainty associated with outcomes of X . The Shannon entropy is one of the central quantities of information theory. For more, see e.g., Ref. 40. It is standard in information theory to use base-2 logarithms for the entropy, while in physics, where the entropy is usually arrived via Eq. (2), one almost always uses natural logarithms. Except as noted below, we will use

base-2 logarithms, and as such are measuring entropy in units of bits.

The entropy density for a two-dimensional system is then defined in the natural way. Consider an infinite 2D lattice of random variables S_{ij} whose values range over the finite set \mathcal{A} . Assuming that the variables are translationally invariant, the 2D entropy density is given by

$$s = \lim_{N, M \rightarrow \infty} \frac{H(N, M)}{NM}, \quad (9)$$

where $H(N, M)$ is the Shannon entropy of an $N \times M$ block of spin variables. (For a triangular lattice, this block may be pictured as a parallelogram.) This limit exists for a translationally invariant system, provided that the limits are taken in such a manner that the ratio N/M remains constant and finite. It is common in information theory and dynamical systems to use h_μ to denote the entropy density. For a dynamical system or stochastic process which unfolds in time and not space, h_μ is referred to as the entropy rate.

Taken together, Eqs. (8) and (9) constitute the familiar Gibbs expression for the entropy density of a two-dimensional lattice system. Equation (9) is slow to converge in N and M and so is of limited practical use. However, there is an alternative expression for s which converges much faster and proves to be very accurate. Moreover, we shall see that this form of the entropy density allows us to decompose the global entropy of the system into local contributions and will also yield a measure of spatial structure or memory. We sketch this method below. For a further discussion, see Ref. 8.

First, we define the *conditional entropy*

$$H[X|Y] \equiv - \sum_{x \in \mathcal{X}, y \in \mathcal{Y}} \Pr(x, y) \log_2 \Pr(x|y), \quad (10)$$

where Y is a random variable that assumes the values $y \in \mathcal{Y}$. The conditional entropy $H[X|Y]$ measures the average uncertainty associated with variable X , if we know the outcome of Y . We now turn our attention momentarily to a one-dimensional system, as it is easier to define the following quantities in 1D. Once their 1D definition is explained, we will discuss their extension to 2D.

In one dimension, the entropy density s may be written as

$$s = \lim_{L \rightarrow \infty} s(L), \quad (11)$$

where

$$s(L) \equiv H[S_L | S_{L-1} S_{L-2} \cdots S_0]. \quad (12)$$

In words, $s(L)$ is the entropy of a single spin conditioned on L of its nearest neighbors. The entropy density is the entropy of this single spin in the limit that it is conditioned on an infinitely long block of neighboring spins. The entropy density s thus represents the average uncertainty per spin, in the limit that correlations over longer and longer blocks of neighboring spins are accounted for.

Examining the manner in which $s(L)$ converges to the entropy density s reveals information about the structure or complexity of the system. The quantity $s(L)$ converges to s from above; for finite L , the system appears more random than it actually is. Summing up these finite- L overestimates gives one the excess entropy, defined via

$$E \equiv \sum_{L=1}^{\infty} (s(L) - s). \quad (13)$$

The excess entropy is thus a measure of the total amount of randomness that is apparent at small length scales that can be “explained away” by considering correlations over larger and larger spin blocks. Thus, the excess entropy captures a structural property of the system; highly structured systems will appear random at small scales but will be less so at larger scales. The excess entropy is a quantity that is complementary to the entropy density. The former is a measure of structure or pattern, while the latter measures randomness or unpredictability.

The excess entropy is a well understood and commonly used measure of structure or complexity for 1D systems. For recent reviews and further discussion, see Refs. 6, 7, 41, 42. The excess entropy is also known as the effective measure complexity^{43,44} and the predictive information.^{6,45} The excess entropy should not be confused with the quantity of the same name that refers to the jump in entropy at a first-order phase transition.

C. Entropy density and excess entropy for two-dimensional systems

We now briefly discuss generalizing Eqs. (11) and (13) to 2D systems. For a detailed treatment, see Sec. III of Ref. 8. Looking at Eq. (12), we are immediately faced with a puzzle. How should we construct $s(L)$ so that in the large L limit it converges to s , defined by Eq. (9)? In 1D, there is a unique ordering to the lattice sites and any one site divides the system into two halves. Neither is the case for a 2D lattice. Conditioning on a 1D block of adjacent spins, as in Eq. (12) will underestimate the entropy. Is there a cluster of spins such that the entropy of a single spin, conditioned on that cluster, equals the 2D entropy density?

This question can be answered in the affirmative. The key is to use a shape that extends laterally left and right, but has a notch in it so that the cluster contains half of the nearest neighbors of the spin whose entropy we are interested in. This is illustrated in Fig. 2. Following Ref. 8, call the single spin whose entropy we are interested in the *target spin*. In Eq. (12), the target spin was S_L . Let $s(M)$ denote the Shannon entropy of a single spin conditioned on a neighborhood of M spins. This neighborhood is shown for $M=7$ in Fig. 2. The numbers in the cells in Fig. 2 indicate the order in which the sites are added on to the cluster. For example, for $M=5$, we would have

$$s(5) = H[S_X | S_1, S_2, S_3, S_4, S_5], \quad (14)$$

where the S_i 's are as illustrated in Fig. 2.

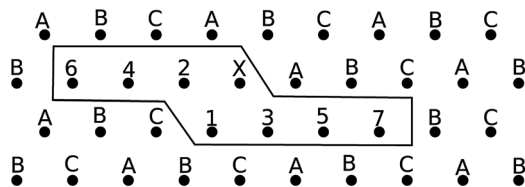


FIG. 2. Target spin (X) and neighborhood templates for conditional entropies. The numbers in the cells indicate the order in which the sites are added to the template. (Compare with Fig. 2 of Ref. 8.)

The entropy density may then be shown to be equal to^{25,28,46,47}

$$\lim_{M \rightarrow \infty} s(M) = s. \quad (15)$$

The clusters of spins we use to form conditional entropies are shown in Fig. 2. Since in our model, the interaction range extends only across one lattice site, the shape need only be one lattice site deep.^{21,22,26,27,46} As a result, an infinitely wide strip has the effect of shielding one half of the lattice from the other.²⁸ In the limit that the strip is infinitely long in the horizontal direction, then the probability distribution of the spin marked with an X is independent of the values of the spins beneath the strip. Note that the shape in Fig. 2 is constructed in such a way that the entropy of the target spin X is conditioned on a neighborhood of spins that includes exactly half of its nearest neighbors. This is achieved by placing a kink in the shape around the target spin. For a further discussion of the motivation behind the shape of Fig. 2, see Sec. III of Ref. 8.

This conditional Shannon entropy method for calculating the entropy density s is well known and has been successfully applied to a wide range of systems.^{24,27,29,48–52} One might expect that this method for estimating the entropy density may work poorly near the critical temperature where there are long range correlations that are missed due to our truncation of M . However, the entropy density estimates converge extremely quickly as a function of M . For example, in Ref. 29, this method is used to find the entropy of the two-dimensional Ising ferromagnet at the critical temperature within 0.01% of the exact value.

If one is interested solely in the entropy of a system, a histogram Monte Carlo approach^{53–56} is competitive with the information theoretic method discussed here. The benefit of the information theoretic method, as we shall see, is that it allows one to decompose the entropy into local contributions, providing a direct way to measure and visualize the “freezing in” that occurs across a spin-glass transition.

Finally, we discuss the excess entropy, Eq. (13), for two-dimensional systems. There are three expressions for the excess entropy, all of which are equivalent in one dimension: the expression in Eq. (13), the mutual information between the system’s past and future, and the sub-extensive scaling term for the block entropy.⁴¹ Each expression leads to a different form for the 2D excess entropy. These forms are not equivalent, but have been shown to behave similarly.⁸ For our work here, we exclusively use the form of excess entropy that arises from Eq. (13), where $s(L)$ is the conditional entropy using the notch shape of Fig. 2. This excess entropy expres-

sion was denoted E_c in Ref. 8. Since, we will only use this form for the 2D excess entropy, we denote it simply by E .

In any event, this form of the excess entropy has been used to study various forms of Ising spin systems.^{8,47,57} This work has shown that the excess entropy is maximized at the critical point of the paramagnet-ferromagnet transition and also that it can serve as a general-purpose measure of spatial structure in two dimensions.

D. Simulation details

To calculate the magnetizations, specific heat, thermodynamic entropy, and local and global information-theoretic entropies, we simulated the Kaya-Berker model using a standard single-flip Metropolis algorithm Monte Carlo simulation. Thus, a time average of our Monte Carlo run corresponds to an average over the canonical ensemble. That is, a configuration c ’s probability of occurrence in the simulation is proportional to $e^{-\mathcal{H}(c)/T}$, where $\mathcal{H}(c)$ is the energy of the configuration c , and T is the temperature. For all the results reported below, we used a system of 98×99 spins and periodic boundary conditions. The system was allowed 4000 Monte Carlo steps (MCS) to equilibrate, sites were updated sequentially, and measurements were taken every 20 MCS. All data reported here are the result of at least 50 000 measurements. We estimated the local entropy densities from block probabilities by observing the frequency of spin-block occurrences. For all of our results, we used a spin block containing a total of 12 spins.

As this system is frustrated, a Monte Carlo simulation will experience glassy behavior at low temperatures; see, e.g., Chapter 6 of Ref. 55. Hence, as the system is cooled, single-spin flip Monte Carlo methods such as those used in our study become inadequate for sampling the whole phase space. The simulation becomes trapped in the vicinity of a local free energy minimum, leading to incorrect sampling probabilities and inaccurate data. An analysis of the correlation time using the auto-correlation function of the Edwards-Anderson order parameter leads us to conclude that $T \approx 0.4$ is the lowest temperature at which our results are reliable; for details see Ref. 58.

There is some controversy as to whether or not various variants of the 2D anti-ferromagnetic Ising model on a triangular lattice show a transition to a spin-glass phase at non-zero temperature.^{1,20,59,60} The goal of this paper is not to investigate the existence, or not, of such a phase transition. Rather, our aim is to explore the properties of local entropy in a frustrated system that experiences glassy behavior. The Kaya-Berker model clearly shows glassy behavior for the finite size systems at the time scales accessible to our Monte Carlo simulation, and hence is well suited for our study. We are not interested in whether or not such behavior persists at longer time scales and in the thermodynamic limit.

IV. RESULTS

A. Comparison with exact results

As a test, we calculated the entropy using the two different methods, Eqs. (2) and (15), for the undiluted case, a pure

antiferromagnet on a triangular lattice. Since the system here is undiluted, it possesses a spatial translation symmetry, and thus, one can obtain the entropy of the system by performing a spatial average over the frequencies of occurrence of spin configurations at different sites.

To calculate the entropy using Eq. (2), one needs to integrate down from $T = \infty$, thus requiring a knowledge of the high temperature behavior of the specific heat c . Rather than run our simulation out to very high temperatures, for both the pure and the undiluted cases, we instead made use of a high-temperature expansion to lowest order in β . This high-temperature expansion was then used to estimate the entropy density at $T = 50$. Subsequently, we used the integral form of Eq. (2) to estimate the entropy at lower temperatures. For details, see Sec. 4.3.1 of Ref. 58.

We find excellent agreement between the entropy density calculated using our two methods: information theoretic and thermodynamic. (These results are not shown; see Fig. 25 of Ref. 58). Both methods also are in agreement with the exact, zero-temperature entropy density of 0.323066 (Refs. 31, 61). Using our information theoretic results down to $T = 0.4$, and then extrapolating down to zero temperature assuming an exponential form, we estimate a ground state entropy of 0.3232 ± 0.0004 , in excellent agreement with the exact result. Using the integration method of Eq. (2), we find a ground state entropy of 0.3216 ± 0.007 , again by extrapolating exponentially down to zero temperature. The error bars are larger for this method, since they arise as a cumulative effect of error bars on each specific heat data point as Eq. (2) is numerically integrated. (Note: we are using natural logs for the ground state entropies reported above, to be consistent with the values published in Refs. 31 and 61).

We then turned our attention to the case in which one sublattice is diluted. In Fig. 3, we plot the three sublattice magnetizations as a function of temperature for the case of 15% dilution. The two undiluted sublattices spontaneously magnetize at around $T \approx 0.8$; their magnetizations are opposite in sign and equal in magnitude. The diluted lattice remains unmagnetized but undergoes a spin-glass ordering at the same temperature, as indicated by a non-zero value for the Edwards-Anderson order parameter. (We have not plot-

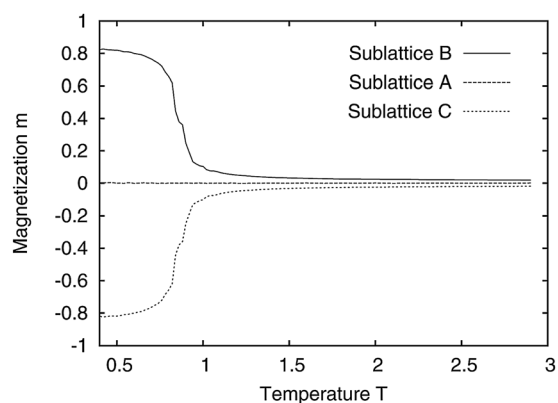


FIG. 3. Sublattice magnetizations plotted as a function of temperature. Sublattice A is diluted at 15%. The two undiluted sublattices, B and C, magnetize with magnetizations that are equal in magnitude and opposite in sign, in agreement with Ref. 1.

ted this result.) The results of Fig. 3 are in excellent agreement with those of Ref. 1.

In this paper, we focus our attention on the model's behavior at 15% dilution. We find that the system's properties are qualitatively similar at other dilutions; for details, see Ref. 58. For 15% dilution, we estimate a critical temperature of 0.84 ± 0.01 . This was obtained by assuming that $m \sim |T - T_c|^\beta$ where β is known to be exactly 1/8. The critical temperature T_c was then varied to obtain the best fit to the calculated magnetizations. For details, see Sec. 5.1 of Ref. 58.

B. Local entropy

The integration method of Eq. (2) can be used for disordered systems without modification. However, in order to use the information theoretic method, Eq. (15), a key modification must be made. In the pure system, one sweeps the template shape of Fig. 2 through the lattice, noting occurrences of each template configuration. The result is the frequency of occurrence of each configuration, averaged over the ensemble (via the Monte Carlo simulation) and averaged spatially over the lattice. However, in a disordered system, if one performs this latter average, one is also averaging over different local regions of diluted sites. In so doing, the randomness of the dilution gets conflated with the fluctuations of the spin degrees of freedom, yielding a significantly overstated entropy for the system.

Instead, we do not sweep our template across the lattice. Rather, we keep the template fixed at a number of selected sites, averaging over the ensemble as our Monte Carlo simulation runs. We thus do not average away the effects of different local bond realizations. The result is a *local* entropy that measures the unpredictability of a particular single spin at a particular site, averaged over the statistical mechanical ensemble. However, this local entropy is not a property of a single site; rather, it takes into account the degree to which a single site is (or is not) correlated with its cluster of neighbors. We will denote these local entropy densities by s_i , where i is a spatial index that labels the site on the lattice. The local entropy tells us how spatially random the system is at that particular site. Spin variables at locations with a low local entropy can be predicted accurately given knowledge of their neighbors, while spins at locations with high local entropy cannot.

In Fig. 4, we show the results of calculating the local entropy at 900 sites for the Kaya-Berker model with 15% dilution. Note that there are a range of different local entropy values. For example, at $T = 1$, there are sites with local entropies as high as around 0.8 and as low as approximately 0.15. The fact that there are multiple local entropy values is a manifestation of the spatial inhomogeneity due to the random dilution of sites on the lattice.

Below $T \approx 0.8$ one can see in Fig. 4 the appearance of forbidden regions in the local entropies; there are ranges of s_i values which no longer occur. Presumably this is due to the fact that there are only a handful of possible local dilution and bond realizations near the target spin. As the system freezes in at low temperatures, target spins with similar local bond and dilution realizations have similar local entropy

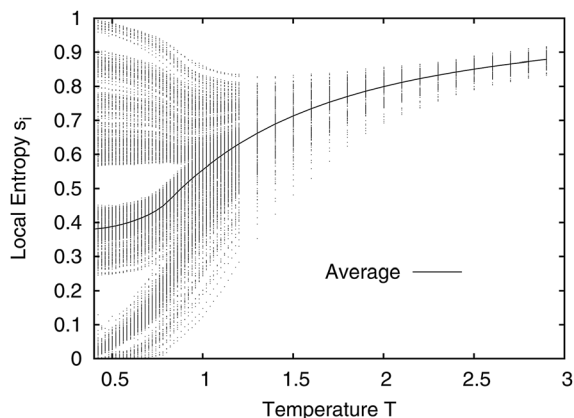


FIG. 4. A sample of the local entropies s_i . The mean of the local entropies is shown as a bold line. The data is “striated” for $T > 1.4$, since in this range measurements were taken at temperature intervals of 0.1. Measurements were taken at intervals of 0.01 below $T = 1.4$. For each temperature, 900 different local entropies are shown for a single 99×98 disorder realization. Plots for different disorder realizations are very similar.

densities, leading to the forbidden regions in Fig. 4. Contrasting behavior is found in a Gaussian spin glass, where bonds assume a continuum of values distributed according to a normal distribution, and thus there are a continuum of local bond environments that a target spin can experience. For such a system the local entropies do not show forbidden regions.⁶²

C. Average of local entropies equals thermodynamic entropy

How are the local entropies s_i related to the entropy of the entire system, given by the thermodynamic integration, Eq. (2)? To answer this question, we average the local entropies. This amounts to a spatial average over the local entropy density values. When forming the average we do not include the local entropies at vacant sites, nor do we count them when normalizing the thermodynamic entropy. That is, the entropy density s is the entropy per *occupied* site.

The results of such an average are shown in Fig. 4 along with the local entropies. In Fig. 5 we have plotted the average of the local entropies together with the thermodynamic entropy obtained via the usual integration. Note the excellent agreement between the spatial average of the local conditional Shannon entropies and the thermodynamic entropy arrived at via an integration over the specific heat, which is a measure of the energy fluctuations in the system.

This agreement indicates that our local entropies s_i may be viewed not only as a local statistic, but as a decomposition of the global, thermodynamic entropy. That is, for a system with N occupied sites:

$$s = \frac{1}{N} \sum_{i=1}^N s_i. \tag{16}$$

Thus, the local entropies capture how the bulk entropy is distributed across the lattice. While we have found strong numerical evidence that the average of the local entropies equals the global entropy—and indeed this seems a natural consequence of the definition of the local entropy—we have not yet

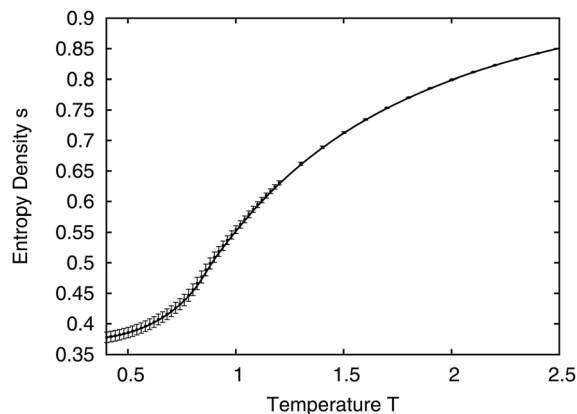


FIG. 5. Comparison of the two methods for calculating the entropy density s . The line is the entropy calculated using the integration method, Eq. (2). The squares are s values calculated using the information theoretic method. Each square is obtained by averaging 22 different disorder realizations. For each disorder realization, the local entropies were calculated for 900 different sites and then averaged. The error bars are the standard deviations for the 22 different averaged local entropies. Note the excellent agreement between the two methods.

obtained an analytic proof of this property. Obtaining a rigorous proof that the two forms of the entropy are equivalent in the thermodynamic limit for an inhomogeneous system such as a spin glass strikes us as a challenging mathematical task and is an important objective for future research.

D. Local excess entropies

We now turn our attention to the excess entropy, defined in Eq. (13). As for the entropy density, we calculate the local excess entropy E_i at a particular site i by keeping our template fixed at site i . The local excess entropies serve as a measure of local structure or memory. The E_i value for a site gives us a measure of how much spatial structure is present at that site; it tells us the amount of apparent randomness that can be “explained away” by taking into account successively larger blocks of its neighbors. As was the case with the local entropy density, the local excess entropy is thus not purely local, in the sense that it is a measure of the extent to which a particular spin shares information with nearby spins.

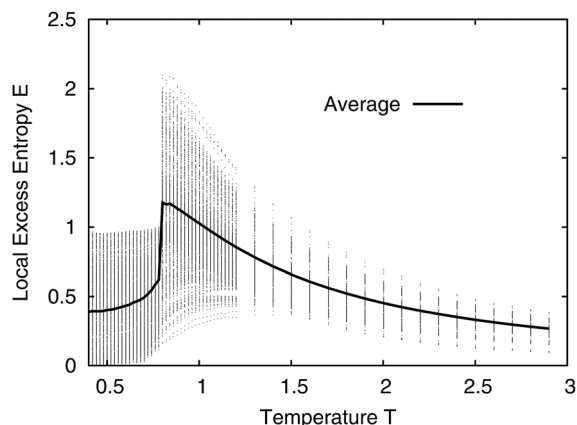


FIG. 6. Local and average excess entropies for the model with 15% dilution. The average excess entropy is indicated by the bold line.

In Fig. 6 we show the results of calculating the local excess entropies at 900 sites. One sees a considerable spread of local excess entropy values E_i . However, note that there do not appear to be any disallowed regions or gaps in the local excess entropies. In contrast, the local entropy density, shown in Fig. 4, shows clear forbidden regions.

We have also plotted in Fig. 6 the average E of the local excess entropy values. Note that the average excess entropy shows a sharp peak. This peak occurs at $T=0.8$. Averaging over 22 different disorder realizations we estimate that the peak value of the excess entropy occurs at $T=0.82 \pm 0.02$.

Estimating T_c using the magnetization, as described in Sec. A yields $T_c = 0.84 \pm 0.01$. We thus conclude that the excess entropy peak coincides with the critical temperature. Further work at other dilutions confirms this general result.⁵⁸ This shows that the excess entropy is a sensitive indicator of the structural changes that the system undergoes at T_c . In contrast, the specific heat (not shown) at the critical temperature is rather rounded,⁵⁸ as is often the case in disordered systems.

The sharpness of the jump in average excess entropy is striking. It has been argued elsewhere^{8,41,63} that the excess entropy E can serve as an all-purpose order parameter. For

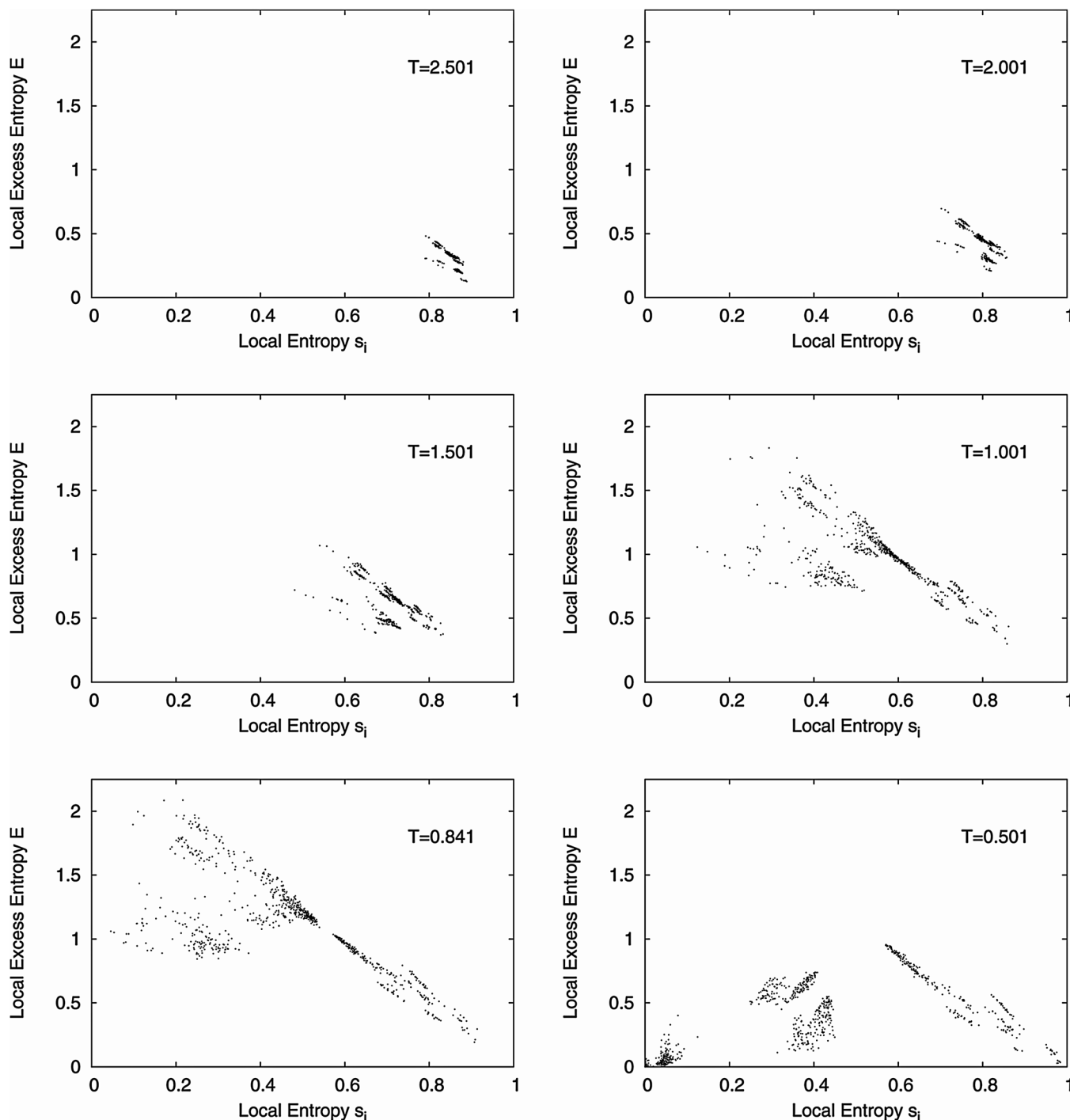


FIG. 7. Local excess entropies plotted against the local entropies for the model with 15% dilution. The temperatures are, top to bottom, left to right, 2.501, 2.001, 1.501, 1.001, 0.841, and 0.501. The complexity entropy diagram for the critical temperature $T \approx 0.841$, is shown in the lower left plot.

example, it has been shown that the excess entropy is sensitive to periodic order of any periodicity. The excess entropy can detect generic structural changes in a system. In contrast, usually order parameters must be tailor-made for a specific type of order. Thus, the use of an order parameter typically requires some *a priori* knowledge of the type of order or structure sought.

The excess entropy requires no such *a priori* knowledge. That the excess entropy detects the phase transition is particularly noteworthy for the Kaya-Berker model studied here. The order parameter for this system actually varies depending on the sublattice: the Edwards-Anderson order parameter is used on the diluted sublattice while the magnetization is used for the other two sublattices. A calculation of the average excess entropy, on the other hand, does not require decomposing the lattice into its three sublattices.

E. Complexity-entropy diagrams

We have seen that at a given temperature there is a range of different local entropy values s_i and local excess entropy values E_i . How are the excess entropy and entropy density values related? Is it the case, for example, that the high entropy sites also have high excess entropy? Is there a full spectrum of s_i and E_i values, or are the two quantities related in some way?

These questions can be addressed with the aid of a construction known as a complexity-entropy diagram,^{57,64} in which a measure of complexity such as the excess entropy is plotted against the entropy density s . This allows one to view a system's computational behavior in terms of parameter-free information processing coordinates. For example, in Ref. 57 complexity-entropy diagrams were calculated for one and two-dimensional Ising models, chaotic maps of the unit interval, cellular automata, Markov chains, and minimal probabilistic automata. The complexity-entropy diagrams allowed for a common framework to view these systems' information processing capabilities without reference to system parameters such as temperature or coupling strength.

In Fig. 7 we plot the complexity-entropy diagram for the Kaya-Berker model for six different temperatures for a single disorder realization. Plots for other disorder realizations appear nearly identical to those of Fig. 7. In the upper left plot, $T = 2.501$ and the system is well above the critical temperature. One sees that a relatively small area of the complexity-entropy diagram is occupied, indicating little information processing diversity. Essentially all sites have a fairly high local entropy density and a low local excess entropy. As the temperature is lowered, the region of occupied complexity-entropy space expands, indicating a greater diversity of local information processing behaviors dispersed across the lattice.

The lower left plot in Fig. 7 shows the complexity-entropy diagram near the critical temperature. Here we see the widest range of information processing behavior. The local entropies range from almost zero (indicating perfect predictability) to almost one (maximally unpredictable).

Note, however, that there is structure evident in this complexity-entropy diagram. In particular, there is a clear

linear upper bound. This phenomenon can be explained as follows. For a 1D Markov chain of order R , there is an upper bound on E as a function of s (see Eq. (15) of Ref. 57):

$$E \leq R(1 - s). \quad (17)$$

The Kaya-Berker model is a 2D system on a triangular lattice. In the template used to form entropy estimates, Fig. 2, the target spin has three nearest neighbors. Thus, the system may be approximated as an order-3 Markov chain. The distribution of the target spin S_x depends almost entirely on the value of the three nearest neighbors. In Fig. 8 we show the complexity-entropy diagram for $T = 0.841$ as well as the upper bound of Eq. (17) with $R = 3$. As expected, this bound is only approximate, since the system is not exactly Markovian. Nevertheless, it captures the form of the upper limit fairly well.

Finally, note the complexity-entropy diagram for $T = 0.501$ in the bottom right of Fig. 7. At this temperature the system is in a glassy, frozen state. Interestingly, the local information processing behavior of the sites seem to be arranged in four clusters. A number of sites have essentially zero entropy density and zero excess entropy, indicating that they are frozen along with their neighbors. However, there are also three clumps on the complexity-entropy diagram that do not have zero entropy. Presumably these sites are not frozen, but instead some degrees of freedom are still active.

As noted above, Ref. 57 calculated the complexity-entropy diagrams for a number of different systems, including 1D and 2D Ising models. The complexity-entropy diagrams of Ref. 57 were obtained by sampling a model class by varying temperature and/or coupling strength. In contrast, complexity-entropy diagrams for the Kaya-Berker model show just one particular instance of the model. Each plot in Fig. 7 corresponds to just one temperature and one disorder realization; the scatter of points represents the range of different local entropies and excess entropies. None of the local complexity-entropy diagrams shown in Fig. 7 show a strong resemblance to those calculated in Ref. 57. This is not surprising; the spin-glass ordering of the sort studied here are generally believed to be structurally quite different from regular Ising models. The information processing coordinates—the entropy density

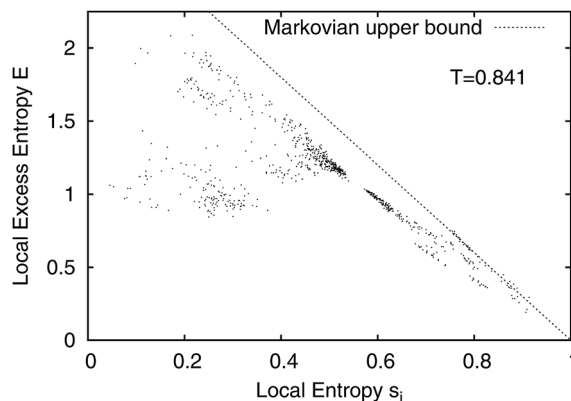


FIG. 8. The complexity entropy diagram for $T = 0.841$. Also shown is the Markovian upper bound, Eq. (17) with $R = 3$.

s_i and the excess entropy E —provide a vivid way to visualize this distinction.

V. DISCUSSION AND CONCLUSION

To summarize, we introduced two local information-theoretic quantities: a local version of the two-dimensional entropy and a local excess entropy. We numerically calculated these quantities for the Kaya-Berker model, a 2D lattice model that shows spin-glass ordering at non-zero temperature. Our main results are as follows.

First, we have presented strong numerical evidence that the entropy of a disordered lattice system can be decomposed into local entropy densities whose mean is equal to the global entropy density. In a heterogeneous system the entropy is not shared equally across the lattice. The local entropies show which sites are more entropic and which are less. We have shown that the model exhibits local reentrance—the local entropy at some sites initially decreases but then increases as temperature is lowered. This result shows that some sites become locally more disordered at lower temperatures, as one might expect in a partially frustrated system with a degenerate ground state.

Second, the local excess entropy can also be divided up into its local contributions. As is the case for the entropy density, sites possess a wide range of local excess entropy values.

Third, the average local entropy shows a sharp, distinct peak at the critical temperature. This provides evidence that the excess entropy, which is already known to be sensitive to periodic ordering,^{8,63} is also a strong indicator of spin glass ordering. The excess entropy is a general measure of pattern or structure, and unlike most order parameters does not require prior knowledge of the relevant pattern.

Fourth, we calculated the local complexity entropy diagrams at different temperatures for the Kaya-Berker model. These diagrams display the range of information processing that is occurring locally across the lattice. The complexity entropy diagrams at lower temperatures reveal a considerable diversity of structure (excess entropy) and unpredictability (entropy density). Moreover, the structure of the complexity entropy diagrams is distinct from those reported in Ref. 57, indicating that frustrated lattice models such as the Kaya-Berker model have a different signature when viewed in information processing coordinates.

We conclude by suggesting several directions for future work. There are a number of ways one can extend and further apply our methods to probe the nature of spin-glass ordering. Other models can be studied, including the Edwards-Anderson spin glass and variants of the random field Ising model. It would be of interest to see if the local information processing behaviors seen for the Kaya-Berker model are similar for other frustrated systems. If so, then this would indicate an information-theoretic feature common across different models. If not, then this would help shed light on the difference between these models.

Another possible extension of our methods would be to form an overlap using the local entropy density. The overlap is a valuable tool for comparison of low-lying energy states in spin glasses. As usually defined, the overlap is a normalized

dot product of average magnetization vectors, in which each vector has as its components the average site magnetizations. A similar overlap function can be defined for the local entropy densities and the local excess entropies. This quantity will demonstrate whether, as the system is cooled, certain regions always retain floppiness while others freeze, or if the locations of these regions vary. This overlap will also show how low-entropy regions become more prevalent under cooling.

The local entropy and excess entropy introduced here may be applied to systems other than spin glasses. Quite generally, these tools can be used to study any lattice system in which information or memory is not shared uniformly across the lattice. Examples include 2D cellular automata and models in which agents interact on a lattice, such as the spatial prisoner's dilemma.^{65,66} Of particular interest might be studying such models on lattices in which some disorder has been added. For example, Vainstein and Arenzon have examined a spatial iterated prisoner's dilemma with deleted sites⁶⁷ and find that doing so increases the fraction of agents that cooperate. This result is tantalizingly similar to what occurs with the Kaya-Berker model, in which site dilution relieves frustration.

The local information theoretic tools introduced here are powerful and broadly applicable. They can be applied to a variety of systems. The result is two quantities—the local entropy density and the local excess entropy—that capture local information processing independent of system parameters. These quantities should find much use understanding the myriad ways that heterogeneous spatial systems store, transmit, and manipulate information.

ACKNOWLEDGMENTS

We thank Jim Crutchfield, Ivan Georgiev, Charles Smith, D. Eric Smith, and Debra Kenneway for helpful discussions. We also acknowledge helpful comments from two anonymous referees. D.P.F. thanks the Santa Fe Institute for their continuing hospitality and for direct support from the Dynamics of Learning group and DARPA contract F30602-00-2-0583.

¹H. Kaya and A. N. Berker, *Phys. Rev. E* **62**, R1469 (2000).

²J. P. Crutchfield, *Physica D* **75**, 11 (1994).

³R. Badii and A. Politi, *Complexity: Hierarchical Structures and Scaling in Physics* (Cambridge University Press, Cambridge, 1997).

⁴C. R. Shalizi and J. P. Crutchfield, *J. Stat. Phys.* **104**, 817 (2001).

⁵C. R. Shalizi, *Methods and Techniques in Complex Systems Science: An Overview*. In T. S. Deisboeck and J. Y. Kresh, editors, *Complex Systems Science in Biomedicine* (Springer-Verlag, New York, 2006), pp. 33–114.

⁶W. Bialek, I. Nemenman, and N. Tishby, *Neural Comput.* **13**, 2409 (2001).

⁷M. Prokopenko, F. Boschetti, and A. J. Ryan, *Complexity* **15**(1), 11 (2009).

⁸D. P. Feldman and J. P. Crutchfield, *Phys. Rev. E* **67**, 051104 (2003).

⁹C. R. Shalizi, K. L. Shalizi, and R. Haslinger, *Phys. Rev. Lett.* **93**, 149902(E) (2004).

¹⁰T. Helvik, K. Lindgren, and M. G. Nordahl, "Local information in one-dimensional cellular automata," in *ACRI 2001, LNCS*, edited by P. M. A. Sloot, B. Chopard, and A. G. Hoekstra (Springer, Berlin/Heidelberg, 2004), Vol. 3305, pp. 121–130.

¹¹C. R. Shalizi, R. Haslinger, J. B. Rouquier, K. L. Klinkner, and C. Moore, *Phys. Rev. E* **73**(3), 036104 (2006).

¹²J. T. Lizier, M. Prokopenko, and A. Y. Zomaya, *Phys. Rev. E* **77**(2), 026110 (2008).

- ¹³K. Young and S. Norbert, *Neuroimage* **39**(4), 1721 (2008).
- ¹⁴J. T. Lizier, M. Prokopenko, and A. Zomaya, *Chaos* **20**(3), 037109 (2010).
- ¹⁵H. Nishimori, *Statistical Physics of Spin Glasses and Information Processing: An Introduction* (Oxford University Press, USA, 2001).
- ¹⁶Z. F. Zhan, L. W. Lee, and J. S. Wang, *Physica A* **285**, 239 (2000).
- ¹⁷J. W. Landry and S. N. Coppersmith, *Phys. Rev. B* **65**(13), 134404 (2002).
- ¹⁸F. Romá, F. Nieto, E. E. Vogel, and A. J. Ramirez-Pastor, *J. Stat. Phys.* **114**(5), 1325 (2004).
- ¹⁹F. Romá, S. Risau-Gusman, A. J. Ramirez-Pastor, F. Nieto, and E. E. Vogel, Ground-state topology of the Edwards-Anderson $\pm J$ spin glass model, <http://arxiv.org/abs/1008.1249>, August 2010.
- ²⁰T. E. Stone and S. R. McKay, *Physica A* **389**(15), 2911 (2010).
- ²¹Z. Alexandrowicz, *J. Chem. Phys.* **55**, 2765 (1971).
- ²²Z. Alexandrowicz, *J. Stat. Phys.* **14**, 1 (1976).
- ²³H. Meirovitch, *Chem. Phys. Lett.* **45**, 389 (1977).
- ²⁴H. Meirovitch, *J. Phys. A* **16**, 839 (1983).
- ²⁵A. G. Schlijper, *Phys. Rev. B* **27**, 6841 (1983).
- ²⁶A. G. Schlijper, A. R. D. van Bergen, and B. Smit, *Phys. Rev. A* **41**, 1175 (1990).
- ²⁷A. G. Schlijper and B. Smit, *J. Stat. Phys.* **56**, 247 (1989).
- ²⁸S. Goldstein, R. Kuik, and A. G. Schlijper, *Commun. Math. Phys.* **128**, 469 (1990).
- ²⁹H. Meirovitch, *J. Chem. Phys.* **111**, 7215 (1999).
- ³⁰J. T. Lizier, M. Prokopenko, and A. Y. Zomaya, A framework for the local information dynamics of distributed computation in complex systems, <http://arxiv.org/abs/0811.2690>, 2008.
- ³¹G. H. Wannier, *Phys. Rev.* **79**, 357 (1950).
- ³²G. S. Grest and E. G. Gahl, *Phys. Rev. Lett.* **43**, 1182 (1979).
- ³³N. Berker, *Physica A* **194**, 72 (1993).
- ³⁴J. F. Fernández, C. Z. Andérico, and T. S. J. Streit, *J. Appl. Phys.* **53**, 7991 (1982).
- ³⁵H. A. Farach, R. J. Creswick, and C. P. Poole, *Phys. Rev. B* **37**, 5615 (1988).
- ³⁶R. J. Crewsick, H. A. Farach, C. P. Poole, and J. M. Knight, *Phys. Rev. B* **32**, 5776 (1985).
- ³⁷C. Z. Andérico, J. F. Fernández, and T. S. J. Streit, *Phys. Rev. B* **26**, 3824 (1982).
- ³⁸R. Netz and A. N. Berker, *Phys. Rev. Lett.* **66**, 377 (1991).
- ³⁹R. Netz and A. N. Berker, *J. Appl. Phys.* **70**, 6074 (1991).
- ⁴⁰T. M. Cover and J. A. Thomas, *Elements of Information Theory* (Wiley, New York, 1991).
- ⁴¹J. P. Crutchfield and D. P. Feldman, *Chaos* **15**, 25 (2003).
- ⁴²W. Ebeling, *Physica D* **109**, 42 (1997).
- ⁴³P. Grassberger, *Int. J. Theor. Phys.* **25**(9), 907 (1986).
- ⁴⁴K. Lindgren and M. G. Norhdal, *Complex Syst.* **2**(4), 409 (1988).
- ⁴⁵I. Nemenman, W. Bialeck, and N. Tishby, *Physica A* **302**, 89 (2001).
- ⁴⁶K. E. Eriksson and K. Lindgren, Entropy and correlations in lattice systems. Technical report No. 89-1, Physical Resource Theory Group, Chalmers University of Technology and University of Göteborg, 1989.
- ⁴⁷K. Lindgren, "Entropy and correlations in discrete dynamical systems," in *Beyond Belief: Randomness, Prediction and Explanation in Science*, edited by J. L. Casti and A. Karlqvist (CRC Press, Boca Raton, Florida, 1991), pp. 88–109.
- ⁴⁸H. Meirovitch, *J. Stat. Phys.* **30**, 681 (1983).
- ⁴⁹H. Meirovitch, *Phys. Rev. B* **30**, 2866 (1984).
- ⁵⁰E. Olbrich, R. Hegger, and H. Kantz, *Phys. Rev. Lett.* **84**, 2132 (2000).
- ⁵¹S. Marcelja, *Physica A* **231**, 168 (1996).
- ⁵²R. L. C. Vink and G. T. Barkema, *Phys. Rev. Lett.* **89**(7), 076405 (2002).
- ⁵³F. G. Wang and D. P. Landau, *Phys. Rev. Lett.* **86**, 2050 (2001).
- ⁵⁴F. G. Wang and D. P. Landau, *Phys. Rev. E* **64**, 056101 (2001).
- ⁵⁵M. E. J. Newman and G. T. Barkema, *Monte Carlo Methods in Statistical Physics* (Oxford University Press, New York, 2000).
- ⁵⁶D. P. Landau and K. Binder, *A Guide to Monte Carlo Simulations in Statistical Physics* (Cambridge University Press, New York, 2000).
- ⁵⁷D. P. Feldman, C. S. McTague, and J. P. Crutchfield, *Chaos* **18**(4), 043106 (2008).
- ⁵⁸M. D. Robinson, "An information theoretic study of the Ising antiferromagnet with quenched vacancies on a triangular lattice," Master's thesis, University of Maine, 2003.
- ⁵⁹T. E. Stone, *Applications of Network Theory to Frustrated Spin Systems and Transitions in Models of Disease Spread*. PhD thesis, University of Maine, 2010.
- ⁶⁰A. A. Middleton, *Phys. Rev. Lett.* **83**(8), 1672 (1999).
- ⁶¹G. H. Wannier, *Phys. Rev. B* **7**, 5017 (1973).
- ⁶²D. A. Kenneway, "An investigation of the two-dimensional Ising spin glass using information theoretic measures," Master's thesis, University of Maine, 2005.
- ⁶³D. P. Feldman and J. P. Crutchfield, Discovering non-critical organization: Statistical mechanical, information theoretic, and computational views of patterns in one-dimensional spin systems. Santa Fe Institute Working Paper 98-04-026, <http://hornacek.coa.edu/dave/Publications/DNCO.html>, 1998.
- ⁶⁴J. P. Crutchfield and K. Young, *Phys. Rev. Lett.* **63**, 105 (1989).
- ⁶⁵M. A. Nowak and R. M. May, *Nature* **359**, 826 (1992).
- ⁶⁶G. Szabo and G. Fath, *Phys. Rep.* **446**(4-6), 97 (2007).
- ⁶⁷M. H. Vainstein and J. J. Arenzon, *Phys. Rev. E* **64**, 051905 (2001).